Chapter 9

Planar Optical Space Switch Architectures

David K. Hunter

Optical space switches are important subsystems in optical crossconnects (OXCs) and reconfigurable optical add/drop multiplexers (R-OADMs), while also having applications in more long-term communications scenarios, such as optical packet switching. This chapter develops the theory of operation of planar optical space switches, and illustrates the inter-relationship that exists between device characteristics, choice of architecture and space switch performance. The chapter also describes how switching elements from a variety of technologies can be combined into larger switch fabrics in different ways.

Recent technological developments such as 3D MEMS, covered elsewhere in this book, have radically changed the performance tradeoff landscape for very large, slow optical crossconnects typically having a reconfiguration time in the order of milliseconds. However, the original vision of interconnected waveguide-based switches still has relevance, especially for sub-nanosecond multiplexing and switching, including the emerging field of fast optical packet switching. Appropriate design can yield fabric performance significantly better than the individual switching elements can separately achieve.

An optical space switch has multiple inputs and outputs, and can establish an optical connection between any idle input and any idle output, without involving conversion of the signal into electronic form. Similar systems, intended for purely electronic implementation, have been studied for over 50 years, and much of that work is amenable to optical implementation. Furthermore, the particular characteristics of optical switches (such as loss, crosstalk and problems of integration) have suggested a number of new architectures which are also discussed here.

Besides describing the optical space switches and their implementation, the theory of their blocking performance is developed. (For further reading on theoretical results in switching, including additional topics such as Banyan networks and Baseline networks, see Reference [1]). Also, formulae are developed for optical loss, crosstalk and noise, which are important aspects of optical space switch performance. This survey is limited to architectures that have actually been built or fabricated, or are strong candidates for implementation in the future.

9-1 Switch models

Before discussing the space switch architectures themselves, the models used to analyze the optical performance of the architectures are introduced.

An $n \times m$ switch has n inputs and m outputs. 1×2 and 2×2 switching devices, which are components of many optical space switches, are often implemented using Lithium Niobate. These are based on interferometric operation under the electro-optic effect, with a switching speed in the order of nanoseconds. Whether based on directional couplers or Mach Zehnder interferometers, as discussed in chapter 2, these devices generally have a periodic response to drive voltage, with an optimal crosstalk only at a single operation point. Device and control tolerancing in conjunction with multiple wavelengths require functionality over an operation

band, reducing the effective crosstalk performance, while strategies to provide polarization independence further limit performance. Devices with saturating responses can significantly reduce these constraints, though the devices are generally larger, with increased electrode capacitance resulting in slower switching speeds. Emerging electro-optic polymer technology may offer new design tradeoffs unavailable with inorganic materials.

Current injection in transparent semiconductor materials (InP, GaAs and Si) provides an alternative way to switch. Switch fabric performance is dependant upon the basic waveguide variability, with InP being most variable and silicon being least. Switching speeds can again be of the order of nanoseconds, depending on the electrical properties. Fiber-to-waveguide losses are generally high in the absence of effective mode tapers, due to the high NA (numerical aperture) of semiconductor waveguides.

Silica technology is another option, dependent on the thermo-optic effect for its operation, with typical switching speeds of a few milliseconds. The low waveguide losses and larger substrate sizes enable complex switch fabrics to be realized. This technology was discussed in chapter 4.

By contrast to the space switches described above, semiconductor optical amplifiers (SOAs) can provide a gating function with extinction ratios beyond 50dB, and with gain to compensate losses in the switch fabric, as discussed in chapter 7.

The first model analyzed here is very much simplified, and is designed to permit a comparison of switch architectures with multiple 2 × 2 devices on one substrate.

The crosstalk in dB of a single 2 × 2 device is represented by X, and its loss (exclusive of any fiber-to-substrate coupling) is L dB. X is always negative. The loss at each fiber/substrate or substrate/fiber interface is W dB. SXR is the signal-to-crosstalk ratio of the whole switching network, while the total insertion loss is A. (In reality, crosstalk terms at the same wavelength as the main signal would produce interferometric noise, which significantly compromises system operation, but this is outside the scope of this chapter. The formulae for signal-to-crosstalk ratio (SXR) developed in this chapter describe the ratio of the desired signal to these interfering terms. The phase noise in the interfering terms is converted to intensity noise when they, and the signal, are converted to electrical form by a square law detector.)

Table 9-1 shows a typical set of values for representative material systems; the set of values for silica is used when comparing architectures in Section 9-11. It is assumed that X and L do not vary for different devices in the same optical space switching system. The model used, excluding waveguide-fiber coupling losses, is shown in Figure 9-1 for the so-called "bar state", (where the signal entering the top (bottom) input exits the top (bottom) output), with[1] $x = 10^{X/10}$ and $l = 10^{-L/10}$. The input/output relationship in the "cross-state" (where the signals cross over in the switch) is similar, except that the outputs are changed over.

[1] These equations are a consequence of the definition of decibels, for example, $X = 10\log_{10}x$.

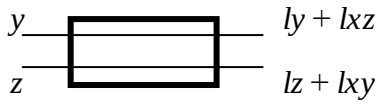

Figure 9-1. Crosstalk and loss model for a directional coupler switch. Multiplication by *l* indicates that loss has occurred due to the switch propagation losses while multiplication by *x* indicates that a signal has gone the "wrong" way in the switch and is now part of a crosstalk term. This model applies primarily to interferometric switches such as directional couplers fabricated in lithium niobate, but not to SOAs.

If a signal enters the space switch and passes through k switches, each of which carries one other signal of identical intensity, the resulting SXR is approximately[2]:

$$SXR \approx -X - 10\log_{10} k \text{ dB} \tag{9.1}$$

The attenuation calculations in this chapter only take account of the loss due to the 2×2 switches and fiber/substrate interfaces. No attempt is made to consider additional waveguide losses, or losses and crosstalk in waveguide bends and crossovers, as the complexity introduced would make the calculations intractable. The equations for attenuation should therefore only be taken as a rough guide.

	X (crosstalk)	*L* (device loss)	*W* (coupling loss)
Lithium Niobate (EO)	–25dB	0.25dB	0.5dB
Gallium Arsenide	–20dB	0.5dB	3dB
Silica (saturating) [2]	–40Db	0.36dB	0.4dB

Table 9-1. Values representing crosstalk and loss for different waveguide-based directional-coupler technologies; used for comparing architectures in section 9-11.

Alternatively, a space switch may be constructed from Semiconductor Optical Amplifiers (SOAs). This may be modeled as a chain of SOAs, since any crosstalk introduced into the fabric is regarded as negligible. The signal-to-noise ratio (SNR) is [3]:

$$\text{SNR} = \frac{\left(G_{sig} P_{in}\right)^2}{4G_{sp} n_{sp} h\upsilon_c B_e \left(G_{sig} P_{in} + G_{sp} n_{sp} \upsilon_c B_o\right)} \tag{9.2}$$

The following notation was used:

P_{in} = signal input power

---

[2] This equation can be derived as follows. *sxr* is the signal-to-crosstalk expressed as a ratio (i.e. not in decibels) and *S* is the signal intensity. Then the intensity of a single crosstalk term will be *xS* and therefore *sxr* = *S*/*kxS* = 1/*kx*. By taking logarithms of both sides and multiplying by 10, one obtains Equation 9-1. When deriving this equation, loss is assumed to be equal for all paths through the network, making the loss for signal and crosstalk terms cancel out. Loss can therefore be assumed to be any value without affecting the result, and may hence be set to zero.

n_{sp} = excess spontaneous emission factor

h = Planck's constant

ν_c = SOA's central frequency

B_e = receiver electrical noise bandwidth

B_o = bandwidth of an optical filter placed on front of the receiver

The signal gain along the chain is:

$$G_{sig} = \left(L_s L_{in} L_{out} G\right)^M \tag{9.3}$$

L_s = system loss in each stage

L_{in} = SOA input coupling loss

L_{out} = SOA output coupling loss

G = gain of one SOA (See equation 7.4, chapter 7).

The spontaneous emission gain is:

$$G_{sp} = \left(\frac{G_{sig}^{1/M}}{L_s L_{in}} - L_{out} \right) \frac{1 - G_{sig}}{1 - G_{sig}^{1/M}} \tag{9.4}$$

In the architectural comparison of Section 9-12, to achieve a 10^{-9} bit error rate (BER), SNR < 144 is required, and the total power leaving the end-face of the last SOA must be less than the nominal saturation power. For further details of this model, see Reference [3].

Having discussed two simple models that may be used to analyze the performance of optical switch fabrics, we now turn our attention to the construction of these fabrics, and the various possible varieties of non-blocking operation.

9-2 Crossbar switches

Originally, crossbar switches were electromechanical devices made up of orthogonal crossbars, with crosspoint switches at the junctions. This formed a rectangular array of crosspoints (Figure 9-2), each of which could connect one of the N input lines to one of the M output lines. This is referred to as an $N \times M$ switch, and is drawn as a box with N inputs and M outputs.

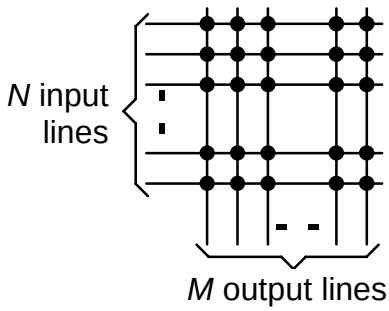

Figure 9-2. An N × *M* crossbar switch.

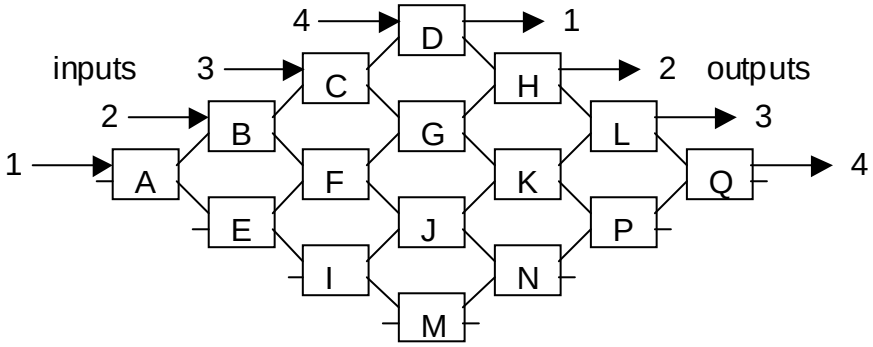

Figure 9-3. A 4 × 4 optical crossbar switch.

Crossbar switches may be implemented optically (Figure 9-3). The diagram shows a 4 × 4 matrix constructed from 16 2 × 2 switches. In general, an $N \times N$ matrix uses N^2 switches, one for each crosspoint. (In the literature on optical switching, the term 'crosspoint' is often used to mean a 2 × 2 switch, regardless of the architecture). The control algorithm is very simple; when no calls are set up, all the switches are set to the cross-state. To connect an idle input to an idle output, the switch that is connected to both is put into the bar-state. To disconnect the call, the same switch is put back into the cross-state. For example, to connect input 2 to output 3, switch J would be put into the bar-state.

From Figure 9-3, one can see that the minimum path length through the switch matrix is one switch (input 4 to output 1), and the maximum is $2N-1$ switches (input 1 to output 4). So the minimum value of insertion loss A is $L + 2W$ and the maximum is $L(2N - 1) + 2W$. While this does mean that the attenuation through the matrix is not constant, the variation is not so marked as it appears from these rough calculations. This is because the attenuation is equalized to some extent by the varying lengths of waveguide required to reach the matrix itself from the edge of the substrate.

In Figure 9-3, the worst possible signal-to-crosstalk ratio occurs when a signal enters on input 1 and leaves on output 1. This is because the maximum number of other signals (i.e. 3) can pass through the switches B, C, and D, which are used by the signal in question. Neglecting loss in the switches:

$$SXR \approx -X - 10\log_{10} 3 \tag{9.5}$$

And for general N,

$$SXR \approx -X - 10\log_{10}(N-1) \tag{9.6}$$

A more accurate formula, which considers the switch attenuation, is [4]:

$$SXR = -X - NL - 10\log_{10}\left(\frac{1-10^{\frac{-(N-1)L}{10}}}{1-10^{\frac{-L}{10}}}\right) \tag{9.7}$$

As $L \to 0$, it reduces to the previous equation; for a comparison of L and W, refer to Table 9-1.

There were several early implementations of this architecture using the electro-optic effect in lithium niobate, for example an 8 × 8 device [5]. Directional coupler switch devices are very much longer than they are wide. In addition, there are limits on the minimum possible waveguide bend ratio that yields an acceptable loss. For these two reasons, the size of crossbar that can be implemented on one substrate is limited.

An OXC based on "delivery and coupling" switches has been proposed [6]. A delivery and coupling switch is essentially a SOA crossbar switch which has the facility to combine many inputs on different wavelengths and send them to one output. The feasibility of its 8 × 16 "delivery and coupling" switch boards for providing 320Gb/s throughput has been confirmed [7]. An architecture derived from the crossbar, made from 2 × 2 devices, has been proposed, having an equal insertion loss for all paths [8]. A 16 × 16 switch of this type, with integrated drive electronics, has been fabricated on one silica substrate. Each 2 × 2 switch operated on the thermo-optic effect. The worst case extinction ratio and loss were 50 dB and 6.7 dB respectively [9].

Routing of 10 Gb/s packets through a compact 4 × 4 InGaAsP/InP vertical coupler SOA crossbar fabric has been demonstrated [10], [11]. The guard band between packets was as short as 2 ns and the adjacent packet suppression ratio was –50 dB.

Crossbars may also be implemented in free space with 2D MEMS (for example, a 16 × 16 device has been fabricated [12].) The switching speed is a few milliseconds, satisfactory for OXC applications, however the minimum and maximum insertion loss may vary by as much as 5 dB due to variable collimation geometry [12].

A 32 × 32 optical crossbar switch called "Champagne" [13] has been reported. It is based upon total internal reflection from the sidewalls of trenches etched in the crosspoints of a silica Planar Lightwave Circuit (PLC) matrix. Normally, liquid is present at a crosspoint, and the light is transmitted straight through. When a small bubble displaces the liquid, light is reflected at the crosspoint.

9-3 Matrix vector multipliers

In *matrix vector multipliers* (MVMs) [3], or broadcast and select switches, each input is connected to every output by means of couplers and an SOA gate that can make or break the connection. There are two variants (Figure 9-4 and Figure 9-5) – the lumped-gain version,

which has only one stage of amplification besides the gates themselves, and the distributed gain version, which has several stages of gain in addition to the gates. Besides any SOAs used purely for amplification, there are N^2 SOAs functioning as on-off gates, where N is the number of inputs and outputs. At most N of these on-off gates are powered at any one time.

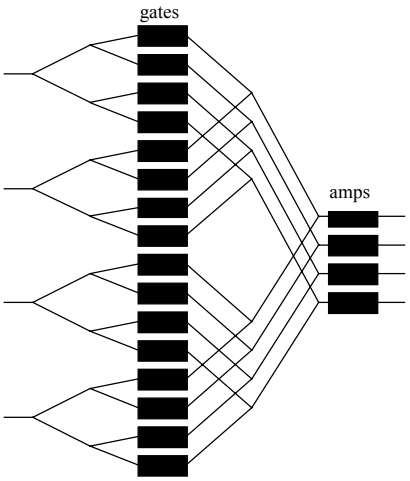

Figure 9-4. An example of a 4 × 4 matrix vector multiplier (MVM) switch with lumped gain. The black rectangles represent SOA gates, which can either be "gates" or amplifiers ("amps").

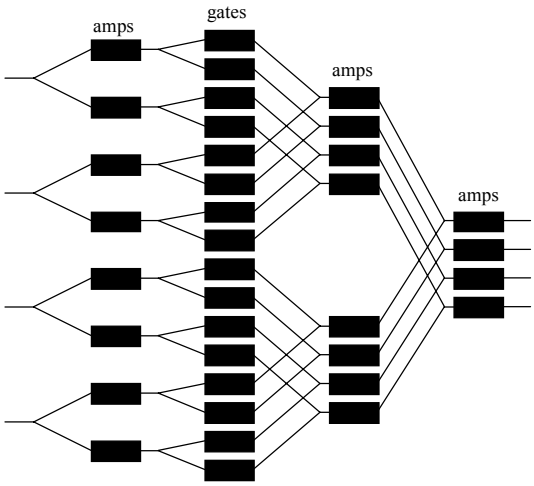

Figure 9-5. An example of a 4 × 4 matrix vector multiplier (MVM) switch with distributed gain. The black rectangles represent SOA gates, which can either be "gates" or amplifiers ("amps").

4 × 4 monolithic matrix vector multiplier switches have been fabricated in InGaAsP/InP [14]. This particular example has three stages – a stage of amplification at both the inputs and outputs (4 + 4 SOAs), and a stage of 16 SOAs to implement switching itself.

9-4 Tree-based architectures

Tree architectures [15] are constructed from tree-structured splitters and combiners, hence their name. They exhibit excellent crosstalk performance, but at the expense of using more devices than many other architectures. On the other hand, for N inputs and outputs, a

crossbar, as described in section 9-2, needs $2N - 1$ stages of switch devices, while a tree switch needs only $2\log_2 N$ stages. For a directional coupler implementation, this allows longer devices (having a longer interaction length) and hence lower operating voltages.

An "active" $1 \times N$ splitter (i.e. a switched demultiplexer) may be constructed from 2×2 switches; a 1×8 example is shown in Figure 9-6. One input on each 2×2 switch is left unused. An active combiner (i.e. a switched multiplexer) is simply an active splitter in reverse. Only $\log_2 N$ control signals are required to drive such an active splitter or combiner. This is because, in each stage, only one of the switches is used at once and hence they can all share one control signal.

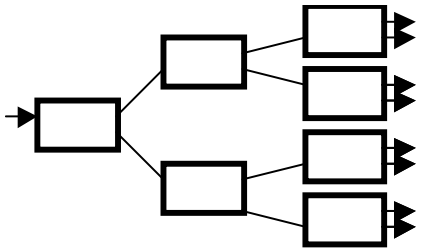

Figure 9-6. A 1 × 8 active splitter.

Corresponding passive splitters and combiners are made from passive fiber couplers, or they may be fabricated with waveguide splitters. The symbols representing splitters and combiners are shown in Figure 9-7. Using a passive splitting or combination stage reduces control complexity but increases loss by a factor of N. In a tree architecture, passive splitting and active combining offers a broadcast function.

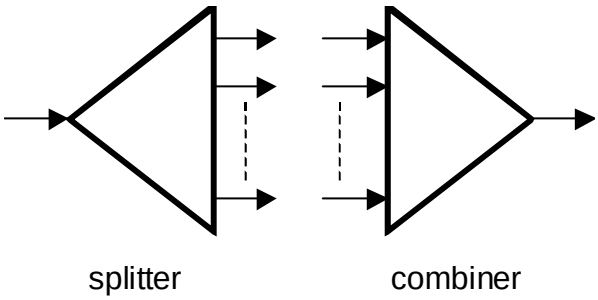

Figure 9-7. Splitter and combiner symbols.

The *tree architecture* itself is shown in Figure 9-8. If active splitters and active combiners are employed, the architecture contains $2N(N-1)$ switches; nearly twice as many as the crossbar switch. The SXR is greatly improved over the crossbar switch, since for a signal to find its way spuriously from an input to a wrong output, it must go to a wrong switch device output, and experience an attenuation of X, at least twice. In fact, the worst-case signal-to-crosstalk ratio is:

$$SXR \approx -2X - 10\log_{10}(\log_2 N) \tag{9.8}$$

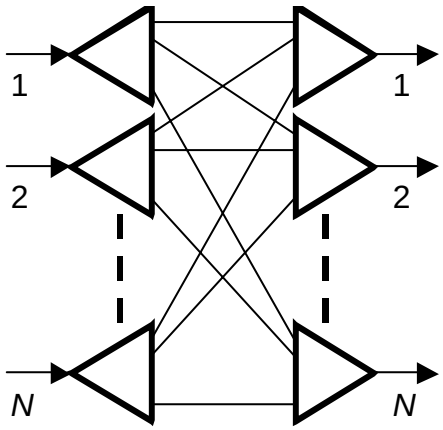

Figure 9-8. The tree architecture.

If the active splitters and combiners are fabricated on separate substrates, the loss is:

$$A \approx 2L \log_2 N + 4W \tag{9.9}$$

If everything is fabricated on one substrate, this becomes:

$$A \approx 2L \log_2 N + 2W \tag{9.10}$$

Clearly, providing a broadcast function will give poorer crosstalk performance.

Polarization independent 4 × 4 implementations of this architecture on single substrates have been reported in lithium niobate, facilitated by the electro-optic effect [16], [17]. A 16 × 16 lithium niobate switch fabric of this type, using multiple substrates with passive splitters and active combiners, was fabricated to act as the center stage of a time-division switching system [18].

A 16 × 16 polymeric device with a tree-based architecture has been fabricated on one substrate, employing the thermo-optic effect [19]. It consists of 480 1 × 2 switches, with 704 S-bends and 227 waveguide intersections. A 1 × 128 multiplexer/demultiplexer on a single silicon substrate has been fabricated, employing the thermo-optic effect [20]. 256 such substrates could be interconnected by fiber to form a 128 × 128 switch.

9-5 Switch fabrics

In the context of optical space switches, a *switching element* is either a 2×2 device or one of the architectures described above; these are connected together to form larger switches called *switch fabrics* (or just *fabrics*). Switch fabrics are organized into *stages*, each consisting of a column of switching elements. In every stage, except for the last one, each switching element output is connected to a switching element input on the next stage. The set of connections between adjacent stages is known as an *interconnect*. The inputs of the first stage switching elements form the input terminals of the switch fabric, and the outputs of the final stage switching elements form the output terminals. All the switch fabrics that are considered here have the same number of inputs as outputs. An example of a three-stage switch fabric is shown in Figure 9-9; stages 1 and 3 are made from 2 × 2 switching elements and stage 2 is

made from 3 × 3 switching elements. It will be assumed throughout the remainder of this chapter that signals travel from left to right through a switch fabric.

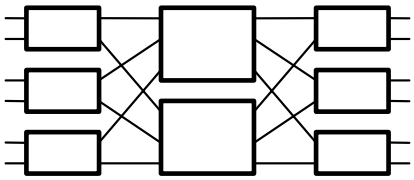

Figure 9-9. An example of a 3-stage switch fabric.

A *call* in a switch fabric is a connection between an input terminal and an output terminal. The switch fabric has a controller associated with it that must be able to accommodate new calls as they arrive, and disconnect old calls once they finish. An *assignment* is a set of calls that are in progress, where each input or output terminal can carry at most one call. An input or output terminal is *free* if it does not carry a call. A *maximal assignment* is an assignment where no input (or output) terminals are free.

A switch fabric is said to be *blocking* if there are one or more assignments that it cannot realize. This is equivalent to saying that it is not always possible to set up a call between a pair of free input and output terminals. Switch fabrics that are not blocking are said to be *nonblocking*; they may be categorized into three types.

In a *strict-sense nonblocking* fabric, there will always be at least one free route through the fabric for a new call, where the call may be set up without rerouting existing calls. Any free route may be used without blocking ever taking place. *Wide-sense nonblocking* fabrics are similar, but some rule must be used to decide what route to choose when activating a new call, otherwise blocking may occur later. In a *rearrangeably nonblocking* fabric, new calls can always be accommodated, but it may be necessary to reroute existing calls through the fabric to do this. The resulting break in service is, of course, unacceptable in an OXC.

This chapter is concerned with strict-sense and rearrangeably nonblocking fabrics. Comparatively little is known about wide-sense nonblocking fabrics, and they will not be considered here to any extent.

9-6 Clos networks

Many switch fabrics are based on a type of three-stage fabric that was first studied by Clos, and are generally referred to as *Clos networks* [21]. The first stage consists of r $n \times m$ switching elements, the second stage m $r \times r$ switching elements, and the third stage r $m \times n$ switching elements (Figure 9-10). Each switch in stages 1 and 2 has exactly one connection to each switching element in the next stage.

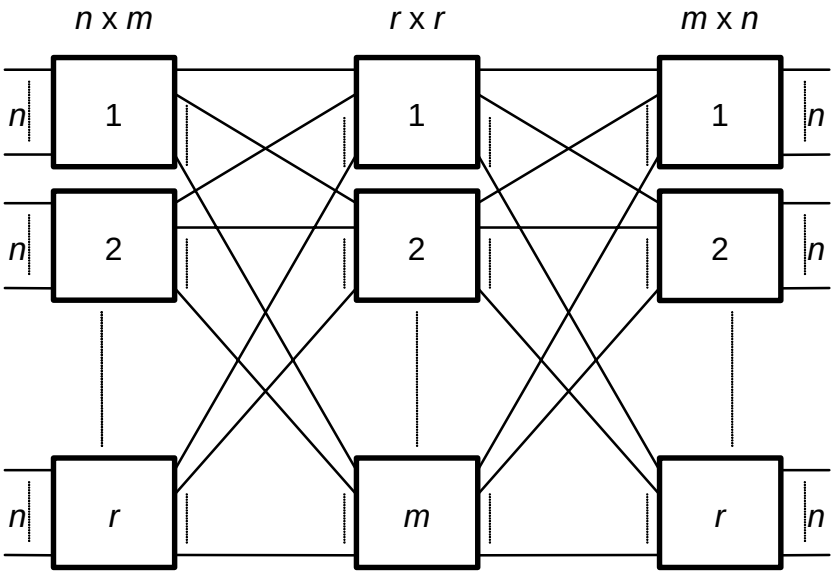

Figure 9-10. A general three-stage Clos network.

If $m \geq 2n - 1$, a Clos network is strict-sense nonblocking [21]. To prove this, it is sufficient to show that, irrespective of how the existing calls are set up, there is always a free path through the network for a new call. Suppose a new call is to be set up between an input on a first stage switching element **A** and an output on an output switching element **B**. The worst case is shown in Figure 9-11; $n - 1$ calls will be already carried through switch **A**, so $n - 1$ center stage switches are used up. Also, $n - 1$ calls pass through **B**, each of them using up a further center stage switch. Since it is the worst case, none of the center stage switches used by calls in **A** are used by calls in **B**. Thus, $2n - 2$ center stage switches are used in the center stage. To provide a free path from **A** to **B**, a further center stage switch must be provided, so there must be at least $2n - 2 + 1 = 2n - 1$ center stage switches.

In the days of early electromechanical systems, the attraction in using this switch architecture, rather than one large crossbar switch, was in the reduction in the number of crosspoints, since this was then a good indication of cost. At the present day, for electronic implementations, this cost reduction benefit has become less pronounced, particularly with the advent of VLSI (Very Large Scale Integration). However, in guided wave optical space switches, the number of switching devices is generally still a good rough estimator of cost.

For large systems, a further reduction in crosspoint count can be made by replacing each center stage switch by another three-stage Clos network, or subnetwork. The resulting network would have five stages. By repeatedly applying this procedure, fabrics with 7, 9, and 11... stages may be produced. As the number of inputs and outputs become larger, the number of stages required to obtain an optimal crosspoint saving increases.

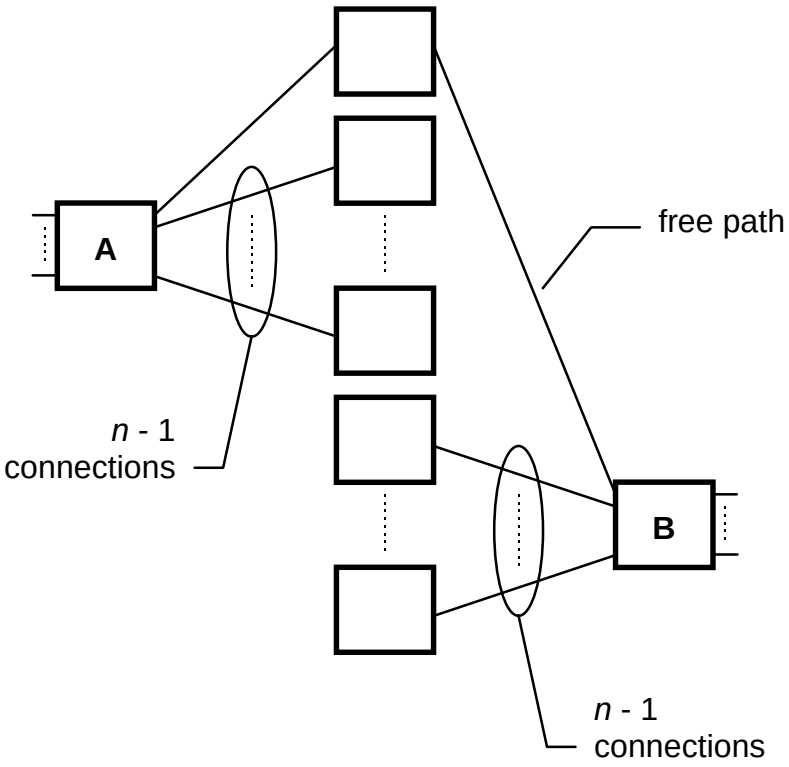

Figure 9-11. The worst-case number of center stage switching elements required in a three-stage Clos network: *m* = 2*n* – 1.

In a $2t+1$ stage network, with $n = \sqrt[t+1]{N}$ throughout, the number of crosspoints $C(2t+1)$ is given by [21]:

$$\begin{aligned}
C(1) &= N^2 \\
C(3) &= 6N^{3/2} - 3N \\
C(5) &= 16N^{4/3} - 14N + 3N^{2/3} \\
C(7) &= 36N^{5/4} - 46N + 20N^{3/4} - 3N^{1/2} \\
C(9) &= 76N^{6/5} - 130N + 86N^{4/5} - 26N^{3/5} + 3N^{2/5} \\
C(2t+1) &= \frac{n^2(2n-1)}{n-1}\left[(5n-3)(2n-1)^{t-1} - 2n^t\right]
\end{aligned} \tag{9.11}$$

It can be shown that this is not the minimum number of crosspoints; for example, for a three-stage network with large *N*, the optimal value of *n* is approximately [21]:

$$n \cong \sqrt{\frac{N}{2}} \tag{9.12}$$

yielding approximately the following number of crosspoints

$$C(3) \cong 4\sqrt{2}N^{3/2} - 4N \tag{9.13}$$

It can be shown that for a three-stage Clos network to be wide-sense nonblocking, $m \geq \lfloor 2n - n/r \rfloor$ [22], where $\lfloor x \rfloor$ is the largest integer less than or equal to x. This result does not specify how a center stage switching element is chosen for each new call i.e. it is the best result possible. If $r = 2$, it holds if a center stage switch which is already in use must, if possible, be assigned to each new call [23]. For large r or small n the saving over strict sense nonblocking is small or non-existent e.g. if $n = 2$ (2×3 switches are used), there is no saving.

To set up a path in such a strict-sense nonblocking fabric, the controller must search iteratively and systematically through possible routes through the network until a free route is found.

A design for a 128×128 photonic switching system has been proposed, implementing a five-stage strict-sense nonblocking Clos network [24]. The system uses lithium niobate electro-optic switching elements, which are based on a variant of the tree architecture, with SOAs to compensate for system losses. The system was not built in its entirety, but experiments were carried out to demonstrate its viability. Several important studies have taken place on the viability of various OXC architectures derived from Clos networks [25], [26].

Moreover, Clos networks have been proposed as a means for interconnecting many small 2D MEMS crossbars to make a large switch fabric [12].

9-7 The Slepian-Duguid theorem

The Slepian-Duguid theorem [23] shows that a Clos network is rearrangeably nonblocking if $m \geq n$. To prove this, it is sufficient to consider a maximal assignment with $m = n$. The theorem does not provide an algorithm for connecting an assignment of inputs onto outputs; it merely states that any such assignment is possible.

This result relies on a combinatorial theorem due to Hall [27], which is often called "Hall's marriage theorem" for reasons that will become clear. It can be stated informally like this. Suppose there are a certain number of boys and the same number of girls, and it is necessary to pair each boy off with a girl that he knows in order to be married. Hall proved that a sufficient and necessary condition for this is that if any group of boys (of size say k) is selected, the number of girls they know between them must be at least k. It is clear that this condition is necessary, but the fact that it is sufficient for the pairing to take place makes the theorem both elegant and surprising.

As an example with $k = 3$, suppose there is a group of 20 boys and 20 girls, and three boys are picked: Brian, Jim and Geoff. Suppose that Brian knows Elaine, Aileen and Jennifer, Jim knows only Elaine and Jennifer and Geoff knows Janice and Elaine. Between them, the three boys know four girls (Elaine, Aileen, Jennifer and Janice), at least as many as the number of boys being considered (three). If all other possible subsets of the 20 boys in the group (there are $2^{20} - 1$ subsets in total) also fulfill such a condition, then Hall's marriage theorem says they may each be paired off with a girl they know. If this were the case, then apart from the other 17 boys, Geoff might marry Elaine, Brian could marry Aileen and Jim could marry Jennifer.

Now consider the Clos network (Figure 9-10). Each of the r boys can be said to "own" a unique input stage switching element and each girl can be said to own a unique output stage switch. A boy is said to know a girl if a call passing through his switching element also

passes through the girl's switching element. Each collection of k boys must know at least k girls, because between them the k boys own switching elements which handle kn calls (remember a maximal assignment is being considered with n calls in each input-stage switching element). These kn calls cannot be distributed over fewer than k output switching elements.

Hence each boy can be paired off with one girl that he knows, and the r calls that this pairing represents (one call for each boy-girl pair) can be routed through the top center stage switching element. This is because one call comes from each input stage switching element and one call goes to each output stage switching element. Now remove this top center-stage switching element from the switch fabric, removing all the calls passing through it, and reduce all the input and output-stage switching elements to $n - 1 \times n - 1$. This reduction in size happens because the inputs and outputs that were occupied by the calls passing through the top center-stage switch are no longer required. Again pair off each boy with a girl that he knows, and continue repeatedly as described above until the entire switch fabric is routed.

9-8 Beneš networks

The Slepian-Duguid theorem can be viewed as showing how smaller fabrics, forming the center stage of a Clos network, can be used to construct a Clos network which is itself a larger fabric. *Beneš networks* [23], [28] are created by repeatedly applying the Slepian-Duguid Theorem in this way. This discussion will be confined to such fabrics built from 2×2 switches, since such devices are readily available. Such fabrics are defined in Figure 9-12, this corresponding to a Clos network with $m = n = 2$, which is rearrangeably nonblocking.

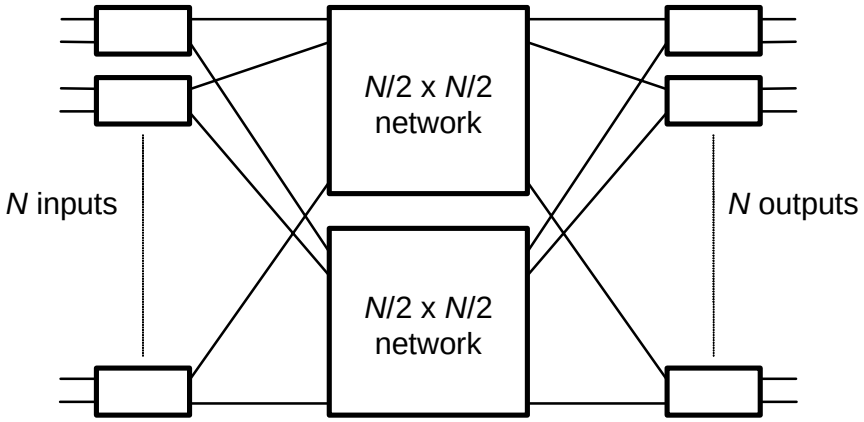

Figure 9-12. Recursive definition of an $N \times N$ Beneš network.

We consider N in Figure 9-12 to be an integral power of 2. If $N = 4$, each center stage switch is a single 2×2 directional coupler switch. If $N > 4$, each center stage switch can be replaced by a $N/2 \times N/2$ Beneš network. By repeating this substitution, a rearrangeably nonblocking Beneš network of arbitrary size can be produced. A Beneš network with 16 inputs/outputs is shown in Figure 9-13.

These switch fabrics are organized into $2\log_2 N - 1$ stages of $N/2$ switching elements; the total number of switching elements required is $N \log_2 N - N/2$. For a more general Beneš

network made from $b \times b$ switching elements, there are $2\log_b N - 1$ stages of N/b switching elements, with $(N/b)(2\log_b N - 1)$ switching elements in total.

The theoretical attenuation for this type of network is:

$$A \approx (2\log_2 N - 1)L + 2W \tag{9.14}$$

The SXR is:

$$SXR \approx -X - 10\log_{10}(2\log_2 N - 1) \tag{9.15}$$

since each signal passes through $2\log_2 N - 1$, 2×2 switches.

Because a Beneš network is rearrangeable, the switch setting may be dramatically changed even if only one new call is set up, which can be as complicated as re-connecting all input-output pairs. The *looping algorithm* is the simplest algorithm to do this [29]. It will be assumed that a maximal assignment is involved, although the algorithm is easily modified if this is not the case.

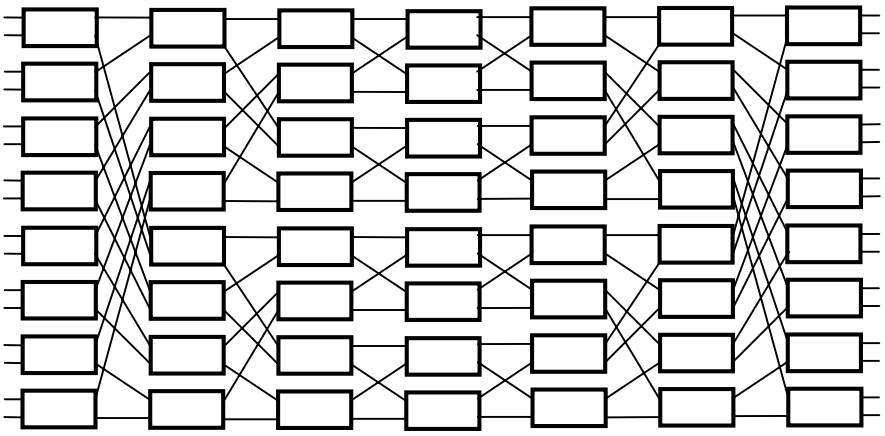

Figure 9-13. A 16 × 16 Beneš network.

Let the inputs be denoted by $u_1, \ldots, u_N$ and the outputs by $v_1, \ldots, v_N$. π is a mapping of the inputs to the outputs, representing a maximal assignment, and π^{-1} is its inverse, mapping outputs onto inputs. For any input u_i, the other input sharing the same first-stage switch is denoted by "co u_i", and similarly, "co v_i" is the output sharing the same output switch as v_i. Initially, all the inputs and outputs are unconnected; the algorithm connects them up as follows, where the variables *S* and *T* represent various inputs and outputs respectively while the algorithm runs:

1. Select any unconnected u_i and set $S = u_i$. If no such input exists then the algorithm terminates since all the inputs are now connected to an output.

2. Connect S to $\pi(S)$ through the top subnetwork in the center stage.

3. Set $T =$ co $\pi(S)$.

4. Connect T to $\pi^{-1}(T)$ via the lower subnetwork in the center stage.

5. Set $S = \text{co } \pi^{-1}(T)$.

6. If S has not been connected to an input, go back to step 2. Otherwise, a "loop" has been completed, so go to step 1 to start a new loop.

The algorithm works by traversing the network between the inputs and the outputs, until it gets back to its starting point, thus forming a loop. An example of a loop, with arrows showing how it was created, is shown in Figure 9-14. Table 9-2 and Table 9-3 show the complete assignment that is to be realized. For each input $u_1,\ldots,u_8$, Table 9-2 shows the corresponding output (one of $v_1,\ldots,v_8$) to which it is to be connected. Table 9-3 relates each output to its corresponding input in a similar way. The loop in Figure 9-14 contains four calls, but a loop may vary in size from two to N calls, and there can be from one to $N/2$ loops, depending on the maximal assignment being realized.

u_i	$\pi(u_i)$
u_1	v_4
u_2	v_2
u_3	v_6
u_4	v_8
u_5	v_5
u_6	v_7
u_7	v_3
u_8	v_1

Table 9-2. Mapping of inputs onto outputs in an 8 × 8 Beneš network.

v_i	$\pi^{-1}(v_i)$
v_1	u_8
v_2	u_2
v_3	u_7
v_4	u_1
v_5	u_5
v_6	u_3
v_7	u_6
v_8	u_4

Table 9-3. Mapping of outputs onto inputs in an 8 × 8 Beneš network.

Calculating the switch settings and subnetwork subassignments in this way takes $O(N)$ time since N calls must be set up sequentially. By applying the algorithm repeatedly for each stage in the Beneš network recursion, routing of a complete fabric (including each subnetwork and their respective subnetworks etc.) can be carried out in $O(N\log N)$ time. The execution time for the algorithm is therefore roughly proportional to $N\log N$. Hence, one of the major disadvantages of a Beneš network compared to other types is the complex control required to accommodate even one new call. It is possible to ameliorate this situation to some extent by employing parallel processors [30], although the algorithm does not adapt to

parallel implementation very efficiently. The looping algorithm is discussed further in chapter 10.

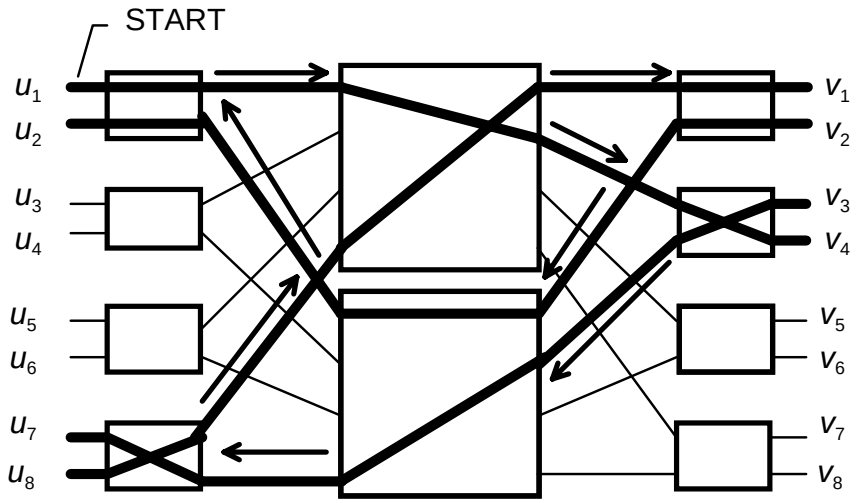

Figure 9-14. One loop in controlling a Beneš network.

Although a 16 × 16 polarization dependent Beneš network has been fabricated [31] operating by means of the electro-optic effect in lithium niobate, better crosstalk performance can be obtained by dilating the switch architecture using two conjoined chips, as discussed in the next section.

OXC architectures have been proposed, based on acousto-optic tunable filters and wavelength converters that employ difference frequency generation [32], [33]. This is logically equivalent to a Beneš network. A method for constructing OXCs from Fiber Bragg Gratings (FBGs) has been proposed [34], using a Beneš architecture; each FBG is tunable by means of compression applied by a stepper motor.

9-9 Dilated Beneš networks

For switch fabrics built from devices having poor crosstalk performance, the SXR calculated by Equation (9.15) may not be adequate. An obvious way of improving the SXR is simply to use better devices; another way is to dilate the switch fabric. Dilation trades off improved SXR for a greater number of switches [35]. The object of dilation is to modify the switch fabric so that each device only carries one signal at once, drastically reducing crosstalk. Suppose the switch fabric has k stages, numbered left to right from 1 to k; in an 8 × 8 Beneš network (Figure 9-15), $k = 5$. There are two steps to dilation. First, a four-switch structure is substituted for each switch (Figure 9-16), carrying out the same function as a single switch, but only permitting one signal to pass through any of its four switch devices at once. The resulting switch fabric has $2k$ stages (Figure 9-17).

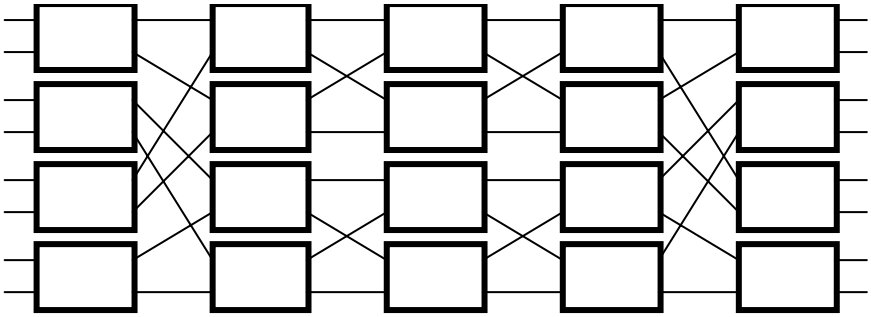

Figure 9-15. An 8 × 8 Beneš network.

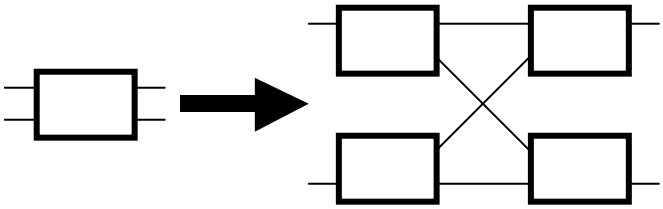

Figure 9-16. First stage in dilating a Beneš network.

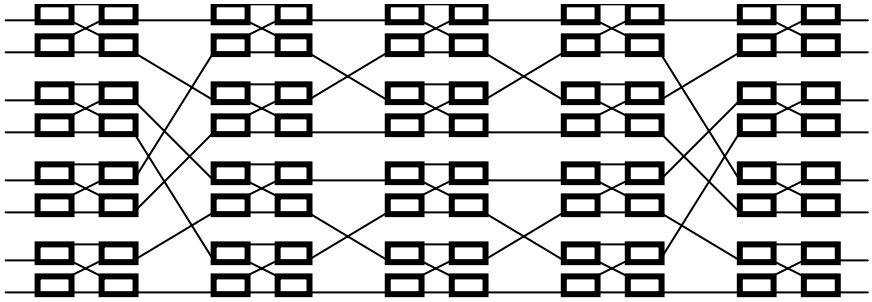

Figure 9-17. An 8 × 8 Beneš network after the first stage of dilation.

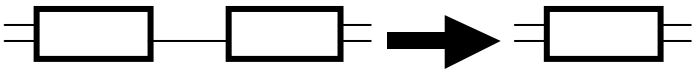

Figure 9-18. The second stage in dilating a Beneš network.

In the second step, each switch device in an even-numbered stage (except the rightmost stage, stage 2*k*) is combined with the switch that it is connected to in the following stage, to form one switch. The required transformation is shown in Figure 9-18; the finished switch fabric has $k + 1$ stages (6 stages in Figure 9-19), and has roughly twice as many switch devices as the original switch fabric. The settings for each switch in a dilated fabric can be derived from those for an undilated fabric by using a small number of logic gates for each switching device.

The theoretical attenuation for this type of switch fabric is:

$$A \approx 2L \log_2 N + 2W \tag{9.16}$$

In reference [35], the crosstalk is described as "negligible"; it is, however approximately [36]:

$$SXR \approx -2X - 20\log_{10}\left(2\log_2 N - 1\right) + 3 \tag{9.17}$$

This figure is over twice as great as the SXR of a conventional Beneš network.

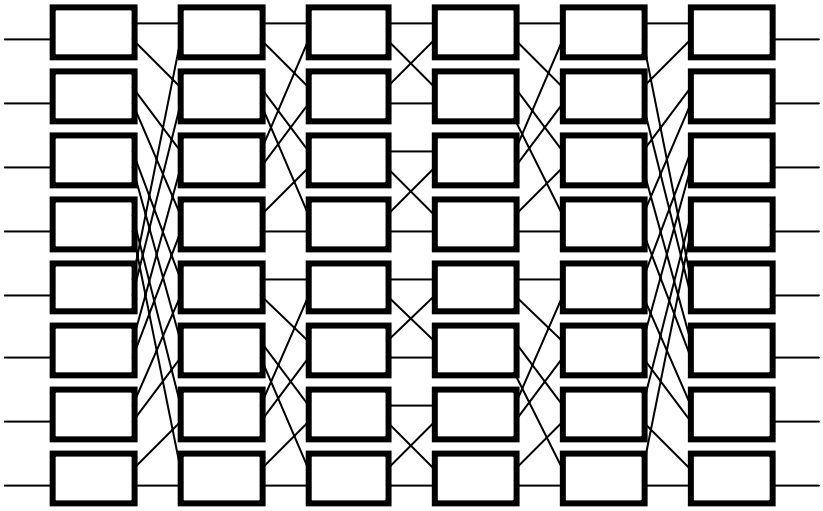

Figure 9-19. An 8 × 8 dilated Beneš network.

Dilated Beneš networks as large as 16 × 16 have been constructed using the electro-optic effect in lithium niobate [37], [38], fabricated as two substrates which were butt-coupled together.

9-10 Stacked switch fabrics

To improve the performance of a switch fabric, for example, by upgrading it from rearrangeably nonblocking to strict-sense nonblocking operation, multiple copies may be stacked in parallel (Figure 9-20). The simplest example of this is the *Cantor network* [39]. Like Clos networks, these are strictly nonblocking. They have the advantage of being constructed from 2 × 2 switching elements, rather than 2 × 3 or 3 × 5 etc. as for strict-sense nonblocking Clos networks. They are constructed from two half networks each named $L(i)$, where i is an integer related to the size of the network. $L(i)$ may be defined as follows. $L(i)$ is a network of switching elements which has $a(i)$ inputs and $b(i)$ outputs. These quantities depend on i (and the size of the network $L(i)$), and expressions to derive them will shortly be obtained.

When calculating the number of outputs that can be connected to a free input without disturbing existing calls (i.e. the number of outputs that can be reached from a free input), the worst case involves having all other inputs busy. Hence let $c(i)$ be the number of outputs of $L(i)$ that the free input could be connected to without disturbing the $a(i) - 1$ existing calls. $L(1)$ is defined as a $1 \times M$ demultiplexer (e.g. Figure 9-6), so $a(1) = 1$, $b(1) = M$ and $c(1) = M$. Networks $L(i)$, where $i > 1$, are defined in terms of $L(i - 1)$ in Figure 9-21. From the diagram, $a(i) = 2a(i - 1)$ and $b(i) = 2b(i - 1)$. Suppose, without loss of generality, that the free input in question is on the lower $L(i - 1)$. Then if all the $a(i - 1)$ inputs on the upper $L(i - 1)$ are disconnected, $2c(i - 1)$ outputs on $L(i)$ can be reached from the free input. If these $a(i - 1)$ inputs are connected up again, in the worst case, $a(i - 1)$ outputs of $L(i)$ which could have been reached otherwise will now become unreachable. Therefore $c(i) = 2c(i - 1) - a(i$

– 1). General solutions are: $a(i) = 2^{i-1}$, $b(i) = M2^{i-1}$, $c(i) = M2^{i-1} - (i-1)2^{i-2}$. We now have expressions for the size of $L(i)$ and the number of outputs that can be reached from a free input. These results are now used to derive a condition for the Cantor network to be strict-sense nonblocking.

Now suppose that there is another network $L(j)$ and it is reflected about the vertical axis so that it has $b(j)$ inputs, $a(j)$ outputs, and at least $c(j)$ inputs reachable from a free output. Call this network $L^{-1}(j)$. The outputs of the original $L(j)$ are connected to the inputs of $L^{-1}(j)$ so that the two outputs on one final stage switching element in $L(j)$ connect to the same switching element on the input stage of $L^{-1}(j)$. Each of these $b(j)/2$ pairs of switching elements can be replaced by a single 2×2 switching element; these switching elements form the center stage of the switch fabric produced from $L(j)$ and $L^{-1}(j)$. This switch fabric is the completed Cantor network.

At least $c(j-1)$ of these 2×2 switching elements are reachable from a free input, and $c(j-1)$ from a free output. To ensure that the switch fabric is strict-sense nonblocking, there must be at least one center stage switching element in common, reachable from both the free input and the free output. A sufficient condition for this to happen is that $2c(j-1) > b(j)/2$ since there are $b(j)/2$ 2×2 switching elements in the center stage. This reduces to $M > j - 2$. The number of inputs and outputs is $N = a(j) = 2^{j-1}$ so the condition becomes

$$M > \log_2 N - 1 \tag{9.18}$$

i.e. $\log_2 N$ is the smallest value of M that yields a strictly nonblocking Cantor network. This type of network requires N $1 \times M$ demultiplexers and N $M \times 1$ multiplexers. There are $2\log_2 N - 1$ stages of 2×2 switch devices, each consisting of $MN/2$ such devices i.e. $MN \log_2 N - MN/2$ devices in total.

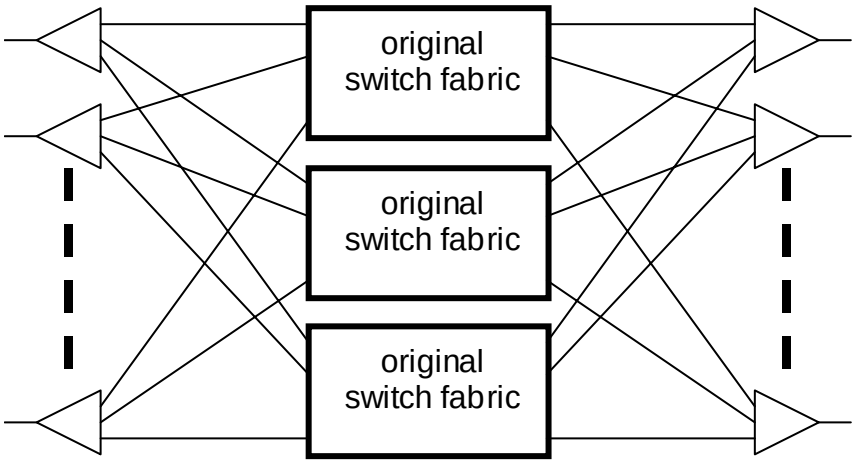

Figure 9-20. A stacked switch fabric, with three copies of the original fabric in this case.

Figure 9-22 is an 8×8 Cantor network. There are many ways in which the switches could be connected up to form such a network; here, the network can be thought of as three 8×8 Beneš networks, 8 demultiplexers and 8 multiplexers. This generalizes, and an $N \times N$ Cantor

network can be constructed from $\log_2 N$ Beneš networks, N demultiplexers and N multiplexers [40].

A type of stacked network, known as the *Extended Generalized Shuffle* (EGS) network has been fabricated from 448 electro-optic lithium niobate directional coupler switching elements in 23 packaged modules [41]. The system was operated continuously and without maintenance for 20 months. EGS networks represent a very general class of switch fabrics, which includes Clos and Cantor networks as special cases.

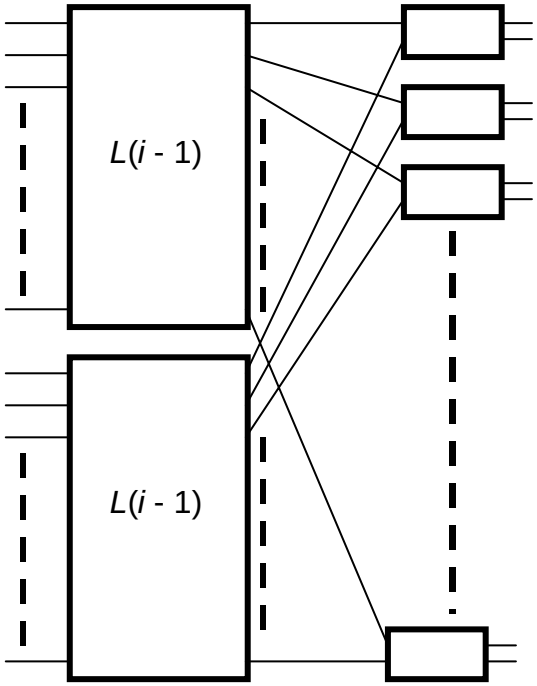

Figure 9-21. Forming a network $L(i)$ from networks $L(i-1)$, when creating a Cantor network.

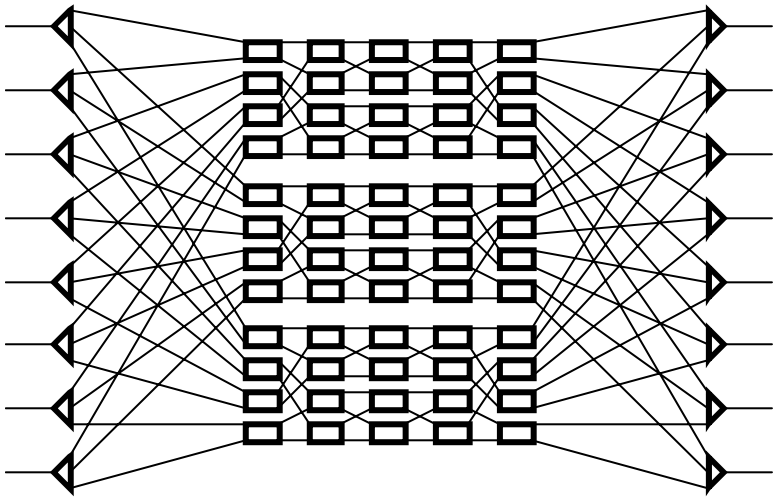

Figure 9-22. An 8 × 8 Cantor network.

9-11 Performance comparison

To conclude, we briefly compare some of the architectures that were introduced above in the context of switch fabrics where switching elements may be cascaded. First, consider those based on SOA gates. In Reference [3], the cascadability of MVM switches was determined analytically, based upon considerations of saturation and signal-to-noise ratio. These findings are summarized here.

Using the model described in Section 9-1, it was found that 200 distributed-gain MVM switches could be cascaded [3], assuming 100 mW SOA saturation power (Figure 9-23). For the purposes of the study saturation powers of 1-100 mW were considered; 100 mW is achievable with quantum well devices [3]. For large switch sizes, the distributed-gain MVM cascades considerably better than the lumped-gain MVM switch, which has gain in only two stages. These figures only take saturation effects into consideration, and in practice, noise would also limit cascadability, with a power penalty of 1 dB for 5-7 cascaded SOAs.

Secondly, Figures 9-24 – Figure 9-26 show the switch device count, SXR and loss for architectures based on thermo-optic silica-on-silicon 2 × 2 switching elements (Table 9-1). The crossbar switch does not scale well in terms of crosstalk or loss, and both the tree and crossbar architectures use a large number of devices, particularly when making a large switch. Hence it is not surprising that these architectures are intended for use as switching elements, since they do not scale to the size generally required for switch fabrics. The tree and dilated Beneš architectures yield the best crosstalk performance. On the other hand, Beneš networks are themselves types of switch fabric so are not designed for use as switching elements. This would in any case be difficult since they are rearrangeably nonblocking and not strict sense nonblocking.

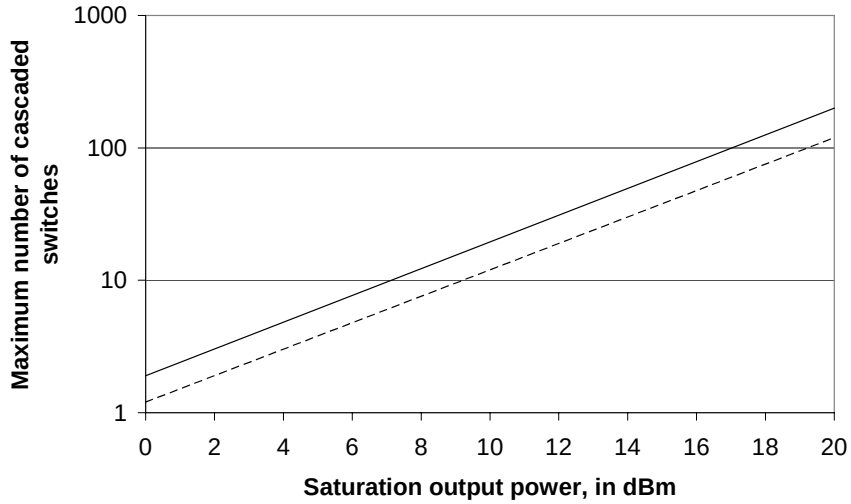

Figure 9-23. Maximum number of 8 × 8 switches that can be cascaded versus saturation output power for distributed-gain MVMs (solid line) and lumped-gain MVMs (dashed line). G_{sig} = 1, B_e = 1 GHz, λ = 1.3 μm, n_{sp} = 5, p_{eff} = 2, L_{in} = L_{out} = 0.5

This chapter has enumerated the main architectural principles behind the design of planar optical space switches. Architectures such as the tree, MVM and crossbar can be used to construct small switching "elements", which are then combined to form larger switch "fabrics". An indication has been given of optical switches found in research laboratories,

and their fabrication technologies, such as lithium niobate directional couplers (and variants), semiconductor optical amplifiers, MEMS, and thermo-optic switches in silica and polymers. While the choice of technology affects performance, it should be clear that the choice of architecture has a significant influence also.

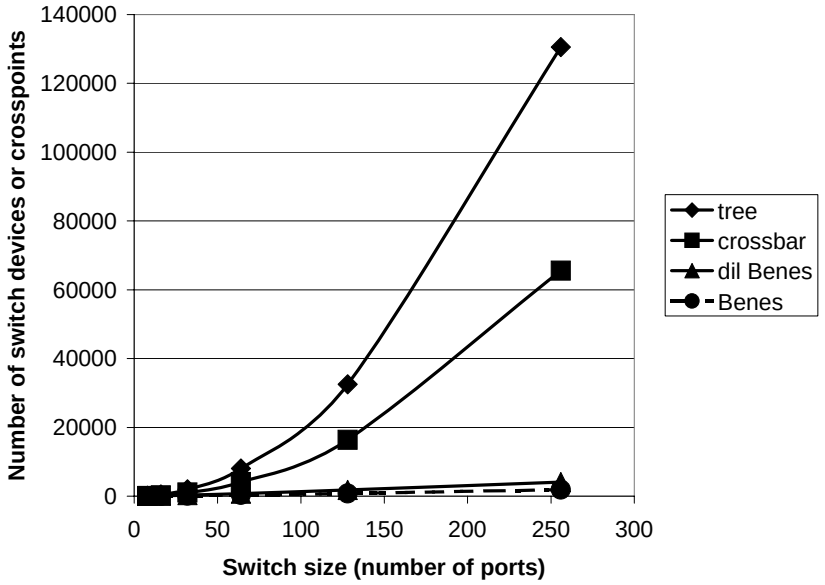

Figure 9-24. Number of switch devices or crosspoints versus number of ports *N* (*N* × *N* architectures are assumed).

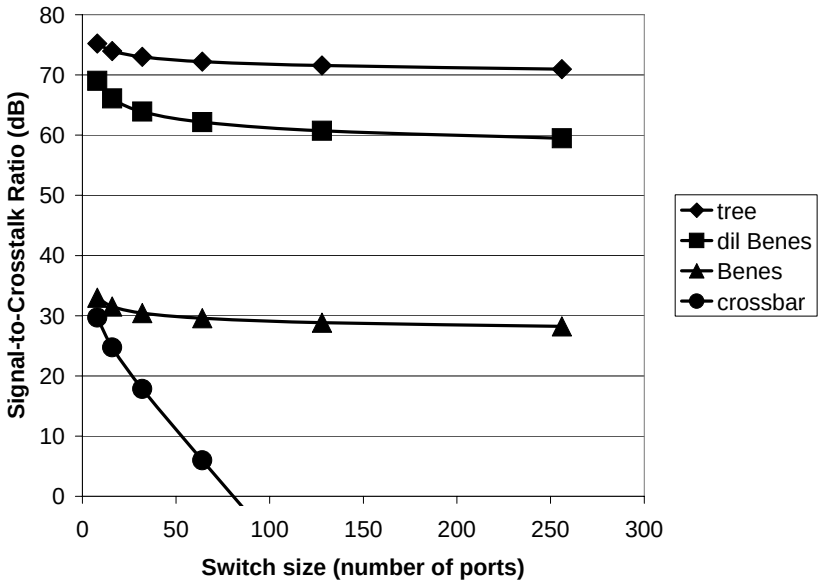

Figure 9-25. Signal-to-crosstalk ratio versus switch size.

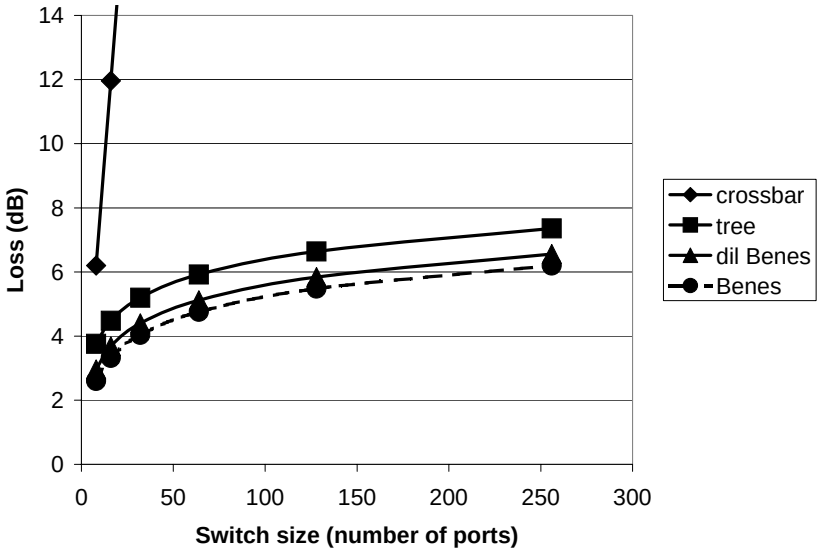

Figure 9-26. Loss versus switch size.

9-12 Acknowledgments

It is a pleasure to thank the following colleagues for reading previous drafts of this chapter, and making many useful and insightful suggestions for improvements:

- Peter Duthie, Madeleine Glick and Sven Östring, all formerly of Marconi Labs, Cambridge, UK,
- Kevin Williams of the Engineering Department, University of Cambridge, UK, and
- Ian Henning of the Department of Electronic Systems Engineering, University of Essex, Colchester, UK.

9-13 References

1. D. K. Hunter: "Switching Systems", *Encyclopedia of Information Technology*, vol. 42, supplement 27, A. Kent, J. G. Williams, C. M. Hall (Eds.), Marcel Dekker, New York/Basel, 2000, pp335-370.

2. T. Goh, M. Yasu, K. Hattori, A. Himeno, M. Okuno, Y. Ohmori: "Low Loss and High Extinction Ratio Strictly Nonblocking 16 × 16 Thermooptic Matrix Switch on 6-in Wafer Using Silica-Based Planar Lightwave Circuit Technology", *IEEE/OSA Journal of Lightwave Technology*, vol. 19, no. 3, March 2001, pp371-379.

3. R. F. Kalman, L. G. Kazovsky, J. W. Goodman: "Space Division Switches Based on Semiconductor Optical Amplifiers", *IEEE Photonics Technology Letters*, vol. 4, no. 9, September 1992, pp1048-1051.

4. H. S. Hinton: "A Nonblocking Optical Interconnection Network Using Directional Couplers", *GLOBECOM 1984*, pp26.5.1-26.5.5.

5. P. Granestrand, B. Stoltz, L. Thylén, K. Bergvall, W. Döldissen, H. Heinrich, D. Hoffman: "Strictly Nonblocking 8 × 8 Integrated Optical Switch Matrix", *Electronics Letters*, 17th July 1986, pp816-818.

6. S. Okamoto, A. Watanabe, K. Sato: "A New Optical Path Crossconnect System Architecture Using Delivery and Coupling Matrix Switch", *Trans. IEICE Japan*, October 1994, vol. E77-B, no. 10, pp1272-1274.

7. A. Watanabe, S. Okamoto, M. Koga, K.-I. Sato, M. Okuno: "Packaging of 8 × 16 Delivery and Coupling Switch for a 320Gb/s Throughput Optical Path Cross Connect System", *IEEE/OSA Journal of Lightwave Technology*, June 1996, vol. 14, no. 6, pp1410-1422.

8. T. Shimoe, K. Hajikano, K. Murakami: "A Path-Independent-Insertion-Loss Optical Space Switching Network", *International Switching Symposium '87*, vol. 4, paper C12.2, pp999-1003.

9. T. Shibata, M. Okuno, T. Goh, M. Yasu, M. Itoh, M. Ishii, Y. Hibino, A. Sugita, A. Himeno: "Silica-based 16 × 16 Optical Matrix Switch Module with Integrated Driving Circuits", *OFC 2001*, Anaheim, CA, March 2001.

10. S. Yu, M. Owen, R. Varrazza, R. V. Penty, I. H. White: "Demonstration of High-Speed Optical Packet Routing using Vertical Coupler Crosspoint Space Switch Array", *Electronics Letters*, 16th March 2000, vol. 36, no. 6, pp556-558.

11. S. Yu, R. Varrazza, M. Owen, R. V. Penty, I. H. White, D. Rogers, S. Perrin, C. C. Button: "Ultra-low Crosstalk, Compact Integrated Optical Crosspoint Space Switch Arrays Employing Active InGaAsP/InP Vertical Waveguide Couplers", *CLEO '99*, post-deadline paper CPD24, Baltimore, 1999.

12. T.-W. Yeow, K. L. E. Law, A. Goldenberg: "MEMS Optical Switches", *IEEE Communications Magazine*, November 2001, pp158-163.

13. J. E. Fouquet: "Compact Optical Cross-Connect Switch Based on Total Internal Reflection in a Fluid-Containing Planar Lightwave Circuit", *OFC 2000*, Baltimore, Maryland, March 2000, paper TuM1.

14. E. Almström, C. P. Larsen, L. Gillner, W. H. van Berlo, M. Gustavsson, E. Berglind: "Experimental and Analytical Evaluation of Packaged 4 × 4 InGaAsP/InP Semiconductor Optical Amplifier Gate Switch Matrices for Optical Networks", *IEEE/OSA Journal of Lightwave Technology*, vol. 14, no. 6, June 1996, pp996-1004.

15. R. A. Spanke: "Architectures for Large Nonblocking Optical Space Switches", *IEEE Journal of Quantum Electronics*, vol. 22, no. 6, June 1986, pp964-967.

16. P. Granestrand, B. Lagerström, P. Svensson, L. Thylén: "Tree-Structured Polarisation Independent 4 × 4 Switch Matrix in $LiNbO_3$", *Electronics Letters*, 15th September 1988, vol. 24, no. 19, pp1198-1200.

17. P. Granestrand, B. Lagerström, P. Svensson, L. Thylén, B. Stoltz, K. Bergvall, J.-E. Falk, H. Olofsson: "Integrated Optics 4 × 4 Switch Matrix with Digital Optical Switches", *Electronics Letters*, 4th January 1990, vol. 26, no. 1, pp4-5.

18. I. M. Burnett, A. C. O'Donnell: "Synchronous Optical Switching in a Time Multiplexed Network", *EFOC/LAN 90, Eighth Annual European Fibre Optic Communications and Local Area Networks Conference*, 27-29 June 1990, Munich.

19. F. L. W. Rabbering, J. F. P. van Nunen, L. Eldada: "Polymeric 16 × 16 Digital Optical Switch Matrix", *ECOC '01*, Amsterdam, postdeadline paper, 2001.

20. T. Watanabe, T. Goh, M. Okuno, S. Sohma, T. Shibata, M. Itoh, M. Kobayashi, M. Ishii, A. Sugita, Y. Hibino: "Silica-based PLC 1 × 128 Thermo-Optic Switch", *ECOC '01,* Amsterdam, 2001.

21. C. Clos: "A Study of Non-Blocking Switch Fabrics", *Bell System Technical Journal,* vol.32,1953, pp406-424.

22. J. C. Boyd, J. M. Hunter, E. McKenzie, D. G. Smith: *Final Report,* Post Office Contract 534325, March 1976.

23. V. E. Beneš: *Mathematical Theory of Connecting Networks and Telephone Traffic*, Academic Press, 1965.

24. C. Burke, M. Fujiwara, M. Yamaguchi, H. Nishimoto, H. Honmou: "128 Line Photonic Switching System using $LiNbO_3$ Switch Matrices and Semiconductor Traveling Wave Amplifiers", *Journal of Lightwave Technology*, vol. 10, no. 5, May 1992, pp610-615.

25. S. Okamoto, A. Watanabe, K.-I. Sato: "Optical Path Crossconnect Node Architectures for Photonic Transport Network", *IEEE/OSA Journal of Lightwave Technology*, June 1996, vol. 14, no. 6, pp1410-1422.

26. H.-H. Witte: "Comparison of a Novel Photonic Frequency-based Switching Network with Similar Architecture", *IEICE Transactions on Communications*, February 1994, vol. E77-B, No. 2, pp157-164.

27. P. Hall: "On Representatives of Subsets", *Journal of the London Mathematical Society,* vol.10, 1935, pp26-30.

28. F. K. Hwang: "On Beneš Rearrangeable Networks", *Bell System Technical Journal,* vol.50, no.1, January 1971, pp20l-207.

29. D. C. Opferman, N. T. Tsao-Wu: "On a Class of Rearrangeable Switching Networks. Part I: Control Algorithm", *Bell System Technical Journal,* vol.50, no.5, May-June 1971, pp1579-1600.

30. G. F. Lev, N. Pippenger, L. G. Valiant: "A Fast Parallel Algorithm for Routing in Permutation Networks", *IEEE Transactions on Computers*, vol. 30, no. 2, February 1981, pp93-100.

31. P. J. Duthie, M. J. Wale, I. Bennion: "Size, Transparency and Control in Optical Space Switch Fabrics: A 16 x 16 Single Chip Array in Lithium Niobate and its Applications", *Technical Digest of the 1990 International Topical Meeting on Photonic Switching*, 12-14 April 1990, Kobe, Japan.

32. N. Antoniades, S. J. B. Yoo, K. Bala, G. Ellinas, T. E. Stern: "An Architecture for a Wavelength-Interchanging Cross-Connect Utilizing Parametric Wavelength Converters", *IEEE/OSA Journal of Lightwave Technology*, vol. 17, no. 7, July 1999, pp1113-1125.

33. N. Antoniades, K. Bala, S. J. B. Yoo, G. Ellinas: "A Paramteric Wavelength Interchanging Cross-Connect (WIXC) Architecture", *IEEE Photonics Technology Letters*, vol. 8, no. 10, October 1996, pp1382-1384.

34. Y.-K. Chen, C.-C. Lee: "Fiber Bragg Grating-Based Large Nonblocking Multiwavelength Cross-Connects", *IEEE/OSA Journal of Lightwave Technology*, vol. 16, no. 10, October 1998, pp1746-1756.

35. K. Padmanabhan, A. N. Netravali: "Dilated Networks for Photonic Switching", *IEEE Transactions on Communications*, vol. 35, no. 12, December 1987, pp1357-1365.

36. D. K. Hunter, D. G. Smith: "New Architectures for Optical TDM Switching", *IEEE/OSA Journal of Lightwave Technology*, vol. 11, no. 3, March 1993, pp495-511.

37. J. E. Watson, M. A. Milbrodt, K. Bahadori, M. F. Bautartas, C. T. Kemmerer, D. T. Moser, A. W. Schelling, T. O. Murphy, J. J. Veselka, D. A. Herr: "A Low-Voltage 8 × 8 Ti:$LiNbO_3$ Switch with a Dilated- Beneš Architecture", *IEEE/OSA Journal of Lightwave Technology*, vol. 8, no. 5, May 1990, pp794-801.

38. T. O. Murphy, C. T. Kemmerer, D. T. Moser: "A 16 × 16 Ti:$LiNbO_3$ Dilated Beneš Photonic Switching Module", *Proceedings of Topical Meeting on Photonic Switching*, Salt Lake City, UT, March 1991, Postdeadline Paper PD3.

39. D. G. Cantor: "On Construction of Nonblocking Switch Networks", *Symposium on Computer Communications Networks and Teletraffic,* Polytechnic Institute of Brooklyn, 4-6 April 1972.

40. G. M. Masson, G. C. Gingher, S. Nakamura: "A Sampler of Circuit Switch Fabrics", *IEEE Computer,* June 1979, pp32-48.

41. E. J. Murphy, T. O. Murphy, A. F. Ambrose, R. W. Irvin, B. H. Lee, P. Peng, G. W. Richards, A. Yorinks: "16 × 16 Strictly Nonblocking Guided-Wave Optical Switching System", *Journal of Lightwave Technology*, vol. 14, no. 3, March 1996, pp352-358.